

## Interaction in the system based on the $\text{Cs}_3\text{Sb}_2\text{Br}_9(\text{I}_9)$ and $\text{Cs}_2\text{TeBr}_6(\text{I}_6)$ compounds

Ivanna STERCHO<sup>1</sup>, Artem POGODIN<sup>1</sup>, Oleksandr KOKHAN<sup>1</sup>, Igor BARCHIY<sup>1\*</sup>, Anatolii FEDORCHUK<sup>2</sup>, Iwan KITYK<sup>3</sup>, Michal PIASECKI<sup>4</sup>

<sup>1</sup> Department of Chemistry, Uzhgorod National University, Pidgirna St. 46, 88000 Uzhgorod, Ukraine

<sup>2</sup> Department of Inorganic and Organic Chemistry, Lviv National University of Veterinary Medicine and Biotechnologies, Pekarska St. 50, 79010 Lviv, Ukraine

<sup>3</sup> Faculty of Electrical Engineering, Technical University, Dabrowskiego St. 69, 42-201 Częstochowa, Poland

<sup>4</sup> Institute of Chemistry, Environment Protection and Biotechnology, Jan Długosz University, Armii Krajowej St. 13/15, 42-200 Częstochowa, Poland

\* Corresponding author. E-mail: i\_barchiy@ukr.net

Received December 14, 2017; accepted December 27, 2017; available on-line April 1, 2018

**The physico-chemical interactions in the system based on the compounds  $\text{Cs}_3\text{Sb}_2\text{Br}_9$ ,  $\text{Cs}_3\text{Sb}_2\text{I}_9$ ,  $\text{Cs}_2\text{TeBr}_6$ , and  $\text{Cs}_2\text{TeI}_6$  were investigated by DTA, XRD and MSA, in combination with mathematical modeling. Due to the formation of an unlimited solid solution in the  $\text{Cs}_2\text{TeBr}_6$ – $\text{Cs}_2\text{TeI}_6$  system, the investigated multicomponent system is presented as the  $\text{Cs}_3\text{Sb}_2\text{Br}_9$ – $\text{Cs}_3\text{Sb}_2\text{I}_9$ – $\text{Cs}_2\text{TeBr}_{6-x}\text{I}_x$  quasiternary system. The projection of the liquidus surface and an isothermal section (573 K) were constructed. The  $\text{Cs}_3\text{Sb}_2\text{Br}_9$ – $\text{Cs}_3\text{Sb}_2\text{I}_9$ – $\text{Cs}_2\text{TeBr}_{6-x}\text{I}_x$  system is of the invariant eutectic type. The crystal structures of the  $\text{Cs}_3\text{Sb}_2\text{Br}_9(\text{I}_9)$  and  $\text{Cs}_2\text{TeBr}_6(\text{I}_6)$  ternary compounds were determined and compared with related B-deficient perovskite structures.**

Halide perovskite / Phase equilibria / Solid solution / Liquidus projection / Crystal structure

### Introduction

The development of modern technologies stimulates the search for new compounds with properties required for the needs of electronic devices. The creation of new functional materials is possible using chemical design methods, which will propose new compounds with more complex compositions and composite materials based on solid solutions. One of the theoretical approaches to study and predict phase equilibria is the method of topological transformation of phase diagrams. It has been successfully used to construct new phase diagrams of ternary and quaternary systems and develop schemes of their topological transformation [1]. The introduction of energy-saving technologies and creation of alternative sources of energy motivate the scientists to search for new photovoltaic materials that can be used in solar cells. The hybrid organic-inorganic halide with a perovskite-type structure  $\text{CH}_3\text{NH}_3\text{PbI}_3$  (power conversion efficiency above 20%) is used in efficient photovoltaic cells [2-5]. However, the internal structural instability of the material and its high toxicity (due to water soluble  $\text{Pb}^{2+}$ ) limits the commercial applications. To eliminate the negative effects on the environment, substitution is carried out in the structure:  $2\text{Pb}^{2+} \rightarrow \text{M}^+ + \text{M}^{3+}$  (the total number

of valence electrons remains constant). Replacement of the  $\text{CH}_3\text{NH}_3^+$  ions in the cationic sublattice by  $\text{Cs}^+$  ions greatly increases the stability of perovskite films [6-8]. Inorganic halide double perovskites of the type  $\text{A}_2\text{B}_1\text{B}_2\text{X}_6$ , based on Bi (In) and Ag, or the vacancy-ordered double perovskite type  $\text{A}_2\text{B}\square\text{X}_6$  (where  $\square$  is a vacancy), show interesting electrophysical properties [9-12].

In order to study the dependence “phase composition – structure – property” for the perovskite-type compounds  $\text{Cs}_3\text{Sb}_2\text{Br}_9(\text{I}_9)$  and  $\text{Cs}_2\text{TeBr}_6(\text{I}_6)$ , we decided to investigate the physico-chemical interactions in the system  $\text{Cs}_3\text{Sb}_2\text{Br}_9 + \text{Cs}_2\text{TeI}_6 \leftrightarrow \text{Cs}_3\text{Sb}_2\text{I}_9 + \text{Cs}_2\text{TeBr}_6$  and analyze the crystal structures of the ternary compounds formed by cation-cation (Sb→Te) and anion-anion (Br→I) substitutions. Modifications of the structure of perovskite phases by iso- and heterovalent substitutions should lead to the emergence of new optoelectronic properties, which opens a prospective for practical use [13,14].

According to Goldschmidt's rule, two empirical quantities, the tolerance factor  $t$  ( $0.86 < t < 1.0$ ) and the octahedral factor  $\mu$  ( $\mu > 0.41$ ) are used to evaluate the crystallographic stability of perovskite-type materials [15]. Calculation of the empirical quantities for the  $\text{Cs}_3\text{Sb}_2\text{Br}_9(\text{I}_9)$  and  $\text{Cs}_2\text{TeBr}_6(\text{I}_6)$  compounds indicates high stability for the individual compounds

and solid solutions based on them with perovskite structure ( $0.91 < t < 0.99$  and  $0.39 < \mu < 0.45$ ) [16].

The Cs<sub>3</sub>Sb<sub>2</sub>Br<sub>9</sub>(I<sub>9</sub>) compounds, formed in the CsBr(I)–SbBr<sub>3</sub>(I<sub>3</sub>) quasibinary systems [17,18], and Cs<sub>2</sub>TeBr<sub>6</sub>(I<sub>6</sub>), formed in the CsBr(I)–TeBr<sub>4</sub>(I<sub>4</sub>) systems [19,20], melt congruently. The systems with substitution of the central anion-forming ion (Sb→Te), Cs<sub>3</sub>Sb<sub>2</sub>Br<sub>9</sub>–Cs<sub>2</sub>TeBr<sub>6</sub> and Cs<sub>3</sub>Sb<sub>2</sub>I<sub>9</sub>–Cs<sub>2</sub>TeI<sub>6</sub>, belong to the eutectic type (V-type diagrams according to Rozeboom) with formation of limited homogeneity regions based on the ternary phases [21,22]. Regarding anion substitution (Br→I), the Cs<sub>3</sub>Sb<sub>2</sub>Br<sub>9</sub>–Cs<sub>3</sub>Sb<sub>2</sub>I<sub>9</sub> system is characterized by eutectic type of interaction [23]. The Cs<sub>2</sub>TeBr<sub>6</sub>–Cs<sub>2</sub>TeI<sub>6</sub> system exhibits the formation of unlimited solid solutions with a minimum of liquidus and solidus lines [24].

## Experimental

The ternary compounds Cs<sub>3</sub>Sb<sub>2</sub>Br<sub>9</sub>, Cs<sub>3</sub>Sb<sub>2</sub>I<sub>9</sub>, Cs<sub>2</sub>TeBr<sub>6</sub>, and Cs<sub>2</sub>TeI<sub>6</sub> were synthesized from stoichiometric amounts of high-purity elemental antimony (99.999 wt.%), tellurium (99.9998 wt.%) bromine (99.99 wt.%), and iodine (99.9998 wt.%), and CsBr and CsI, additionally purified by vacuum melting and direct crystallization. The synthesis was carried out by the two-temperature method in quartz glass ampoules evacuated down to 0.13 Pa. The synthesis was performed in the following regime: heating at a rate of 20–30 K/h up to a temperature exceeding the melting point by 50–60 K (948 K for Cs<sub>3</sub>Sb<sub>2</sub>Br<sub>9</sub>, 926 K for Cs<sub>3</sub>Sb<sub>2</sub>I<sub>9</sub>, 1068 K for Cs<sub>2</sub>TeBr<sub>6</sub>, 886 K for Cs<sub>2</sub>TeI<sub>6</sub>). The heating was accompanied by rotating of the ampoule for saturation. At the maximum temperature (exposure for 72 h), all the components and products of the interaction were in the molten form, which conditioned the completion of the chemical interaction with formation of the desired phases. Cooling to an empirically selected (or selected based on known phase diagrams) annealing temperature was carried out at a rate of 20–30 K/h. The annealing temperature and duration (168–240 h) were selected for each compound individually.

Twenty-seven samples were synthesized from the original ternary compounds by direct fusion in evacuated quartz glass ampoules. The synthesis was performed in the following regime: heating at a rate of 50 K/h up to 1035 K, aging at this temperature for 48 h, and cooling (50 K/h) to the annealing temperature at 573 K (240 h). Subsequently the ampoules were quenched in cold water.

The phase equilibria were studied by differential thermal analysis (DTA), X-ray powder diffraction (XRD) and microstructure analysis (MSA), in combination with the simplex method of phase equilibria computer simulation. DTA was carried out using a chromel–alumel thermocouple with an accuracy of  $\pm 5$  K and automatic data recording. The

samples were heated and cooled in a furnace using an RIF-101 programmer, which provided a linear temperature variation. XRD was carried out on a DRON-4 diffractometer (Cu K $\alpha$  radiation, Ni filter). MSA was executed on a LOMO Metam R-1 metallographic microscope. The mathematical method of phase equilibria modeling in multi-component systems is described in [25].

## Results and discussion

Based on the DTA it was found that the ternary complex compounds melt congruently at 864 K (Cs<sub>3</sub>Sb<sub>2</sub>Br<sub>9</sub>), 876 K (Cs<sub>3</sub>Sb<sub>2</sub>I<sub>9</sub>), 1019 K (Cs<sub>2</sub>TeBr<sub>6</sub>), and 806 K (Cs<sub>2</sub>TeI<sub>6</sub>). The Cs<sub>3</sub>Sb<sub>2</sub>Br<sub>9</sub> ternary compound is characterized by a polymorphic transformation at 791 K (Fig. 1).

The topology of the phase relations in the quaternary system considers the interaction in the binary and ternary systems. According to the fact that an unlimited solid solution is formed in the Cs<sub>2</sub>TeBr<sub>6</sub>–Cs<sub>2</sub>TeI<sub>6</sub> quasibinary system and can be considered as one component, Cs<sub>2</sub>TeBr<sub>6-x</sub>I<sub>x</sub>, the investigated system may be presented as the Cs<sub>3</sub>Sb<sub>2</sub>Br<sub>9</sub>–Cs<sub>3</sub>Sb<sub>2</sub>I<sub>9</sub>–Cs<sub>2</sub>TeBr<sub>6-x</sub>I<sub>x</sub> quasiternary system.

Based on the results of DTA, XRD and MSA, and using computer simulation of phase equilibria in multi-component systems, the projection of the liquidus surface (Fig. 2a) and the isothermal section at 573 K (Fig. 2b) of the Cs<sub>3</sub>Sb<sub>2</sub>Br<sub>9</sub>–Cs<sub>3</sub>Sb<sub>2</sub>I<sub>9</sub>–Cs<sub>2</sub>TeBr<sub>6-x</sub>I<sub>x</sub> system were constructed. Limited solid solutions are formed in the system:  $\alpha$  based on Cs<sub>2</sub>TeBr<sub>6-x</sub>I<sub>x</sub>,  $\beta$  and  $\beta'$  based on the low- and high-temperature modification of Cs<sub>3</sub>Sb<sub>2</sub>Br<sub>9</sub>, respectively, and  $\gamma$  based on Cs<sub>3</sub>Sb<sub>2</sub>I<sub>9</sub>. Due to the polymorphic transformation of the Cs<sub>3</sub>Sb<sub>2</sub>Br<sub>9</sub> compound that takes place at 720 K in the quasiternary system, the reflections of the high-temperature modification ( $\beta'$ -phase) were not observed in the diffraction patterns of the alloys at 573 K.

The liquidus of the Cs<sub>3</sub>Sb<sub>2</sub>Br<sub>9</sub>–Cs<sub>3</sub>Sb<sub>2</sub>I<sub>9</sub>–Cs<sub>2</sub>TeBr<sub>6-x</sub>I<sub>x</sub> system consists of three fields of primary crystallization:  $\alpha$ -crystals (Cs<sub>2</sub>TeBr<sub>6</sub>–e2–E–e3–Cs<sub>2</sub>TeI<sub>6</sub>),  $\beta'$ -crystals (*htm*–Cs<sub>3</sub>Sb<sub>2</sub>Br<sub>9</sub>–e1–E–e2–*htm*–Cs<sub>3</sub>Sb<sub>2</sub>Br<sub>9</sub>) and  $\gamma$ -crystals (Cs<sub>3</sub>Sb<sub>2</sub>I<sub>9</sub>–e1–E–e3–Cs<sub>3</sub>Sb<sub>2</sub>I<sub>9</sub>). The fields of primary crystallization are separated by three monovariant eutectic lines, e1–E ( $L \leftrightarrow \beta' + \gamma$ , temperature region 810–737 K), e2–E ( $L \leftrightarrow \alpha + \beta'$ , 830–737 K) and e3–E ( $L \leftrightarrow \alpha + \gamma$ , 772–737 K). The monovariant lines cross in the invariant eutectic point E:  $L \leftrightarrow \alpha + \beta' + \gamma$ , 737 K (26 mol.% Cs<sub>3</sub>Sb<sub>2</sub>Br<sub>9</sub>, 32 mol.% Cs<sub>3</sub>Sb<sub>2</sub>I<sub>9</sub>, 19 mol.% Cs<sub>2</sub>TeBr<sub>6</sub>, 23 mol.% Cs<sub>2</sub>TeI<sub>6</sub>). The microstructure of a ternary alloy (30 mol.% Cs<sub>3</sub>Sb<sub>2</sub>Br<sub>9</sub>, 31 mol.% Cs<sub>3</sub>Sb<sub>2</sub>I<sub>9</sub>, 19 mol.% Cs<sub>2</sub>TeBr<sub>6</sub>, 20 mol.% Cs<sub>2</sub>TeI<sub>6</sub>) in the three-phase region  $\alpha + \beta + \gamma$  near the eutectic point is presented in Fig. 3. Formation of new complex quaternary compounds was not observed in the Cs<sub>3</sub>Sb<sub>2</sub>Br<sub>9</sub>–Cs<sub>3</sub>Sb<sub>2</sub>I<sub>9</sub>–Cs<sub>2</sub>TeBr<sub>6-x</sub>I<sub>x</sub> system.

We confirmed the crystal structures and studied the relations between the perovskite structures of the Cs<sub>3</sub>Sb<sub>2</sub>Br<sub>9</sub>(I<sub>9</sub>) and Cs<sub>2</sub>TeBr<sub>6</sub>(I<sub>6</sub>) ternary compounds. The relation between the perovskite phases can be represented by the scheme Cs<sub>6</sub>[Sb<sub>4</sub>□<sub>2</sub>]Br<sub>18</sub>(I<sub>18</sub>) ↔ Cs<sub>6</sub>[Sb<sub>4-x</sub>Te<sub>3x/4</sub>□<sub>2+x/4</sub>]Br<sub>18</sub>(I<sub>18</sub>) ↔ Cs<sub>6</sub>[Te<sub>3</sub>□<sub>3</sub>]Br<sub>18</sub>(I<sub>18</sub>). The crystallographic parameters of the compounds are listed in Table 1.

The crystal structure of ideal perovskite with the general formula ABX<sub>3</sub> is cubic. The atoms A are characterized by a cubo-octahedral environment whereas the atoms B center octahedrons. The octahedrons [BX<sub>6</sub>] are connected by the vertices of the polyhedrons and form an infinite 3D framework. As a result of heterovalent replacement of B atoms, vacant positions in the structure are formed, which leads to the appearance of a number of compounds that are defective derivatives of the perovskite structure.

The crystal structure of Cs<sub>2</sub>TeBr<sub>6</sub>, *cF36*, 225 [29] and Cs<sub>2</sub>TeI<sub>6</sub>, *cF36*, 225 [30], structure type K<sub>2</sub>PtCl<sub>6</sub>, can be represented as the stacking in three directions of cubes formed by Cs atoms. Half of the cubes are filled by anionic groups [TeX<sub>6</sub>]<sup>4-</sup> and the other half are empty (Fig. 4). The coordination octahedrons [TeX<sub>6</sub>] are formed by six halogen atoms X, which are located at the vertices of a regular polyhedron, at the center of which the Te atom is located.

The crystal structure of Cs<sub>2</sub>SbBr<sub>6</sub>, *tI72*, 141 (structure type [NH<sub>4</sub>]<sub>2</sub>SbBr<sub>6</sub> [28]), which may be derived by multiple isovalent substitution 2Te<sup>4+</sup> ↔ Sb<sup>3+</sup>+Sb<sup>5+</sup>, can also be presented as the stacking of empty and filled cubes (Fig. 5). Since the octahedrons [SbX<sub>6</sub>] contain two different types of Sb atom, there is a slight deformation of the polyhedrons, which are tilted with respect to the z-axis.

**Table 1** Crystallographic data of the Cs<sub>3</sub>Sb<sub>2</sub>Br<sub>9</sub>(I<sub>9</sub>), Cs<sub>2</sub>SbBr<sub>6</sub>, and Cs<sub>2</sub>TeBr<sub>6</sub>(I<sub>6</sub>) complex compounds.

Compound	Crystal system	Space group	Lattice parameters
Cs <sub>3</sub> Sb <sub>2</sub> Br <sub>9</sub> [26]	trigonal	<i>P</i> -3 <i>m</i> 1	<i>a</i> = 7.930(1), <i>c</i> = 9.716(9) Å
Cs <sub>3</sub> Sb <sub>2</sub> I <sub>9</sub> [27]	hexagonal	<i>P</i> 6 <sub>3</sub> / <i>mmc</i>	<i>a</i> = 8.349(1), <i>c</i> = 20.9160(10) Å
Cs <sub>2</sub> SbBr <sub>6</sub> [28]	tetragonal	<i>I</i> 4 <sub>1</sub> / <i>amd</i>	<i>a</i> = 10.7320(1), <i>c</i> = 21.7442(2) Å
Cs <sub>2</sub> TeBr <sub>6</sub> [29]	cubic	<i>Fm</i> -3 <i>m</i>	<i>a</i> = 10.918(2) Å
Cs <sub>2</sub> TeI <sub>6</sub> [30]	cubic	<i>Fm</i> -3 <i>m</i>	<i>a</i> = 11.700(4) Å

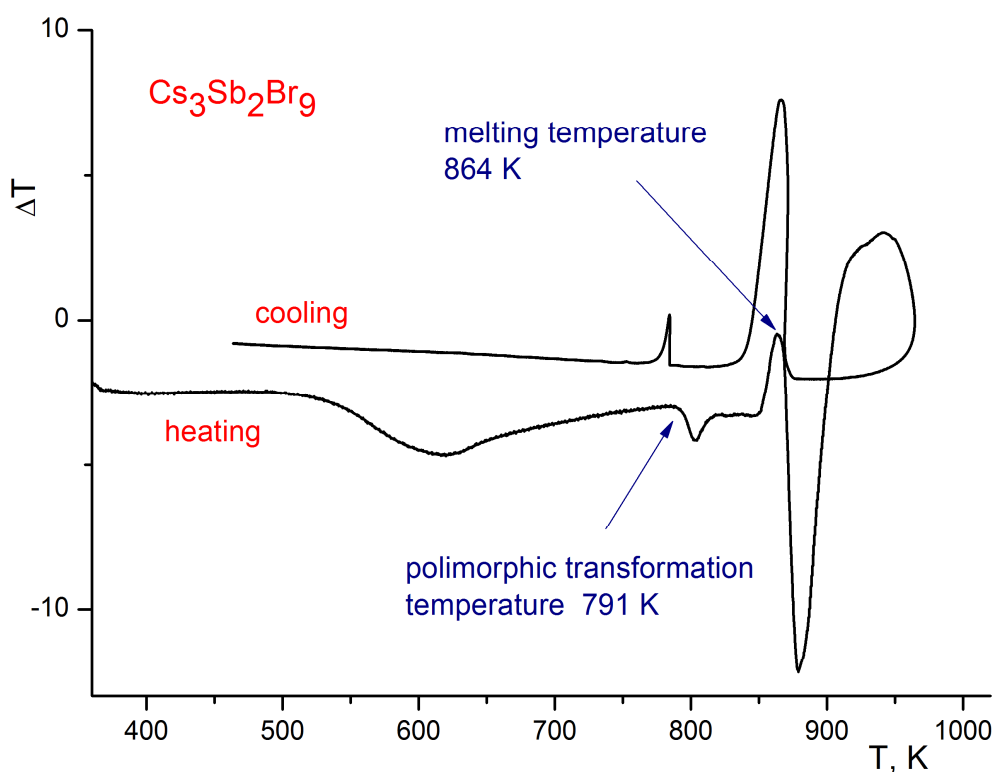


**Fig. 1** Results of the DTA investigation of the Cs<sub>3</sub>Sb<sub>2</sub>Br<sub>9</sub> compound.

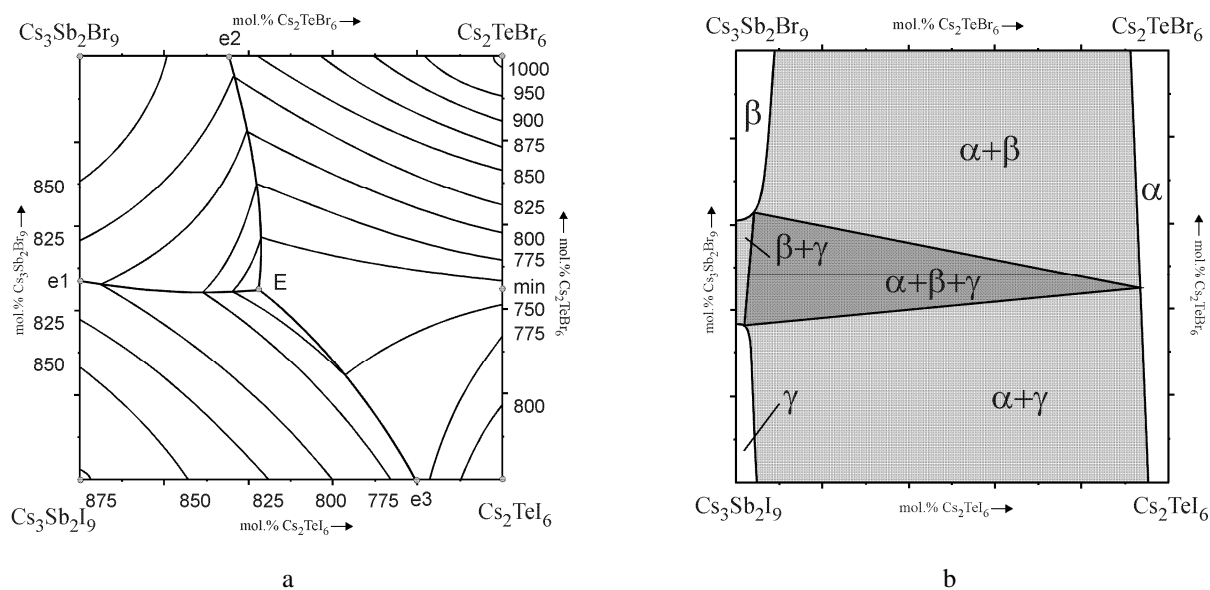


**Fig. 2** Liquidus surface projection (a) and isothermal section at 573 K (b) of the  $\text{Cs}_3\text{Sb}_2\text{Br}_9$ – $\text{Cs}_3\text{Sb}_2\text{I}_9$ – $\text{Cs}_2\text{TeBr}_6$ – $\text{I}_x$  system.

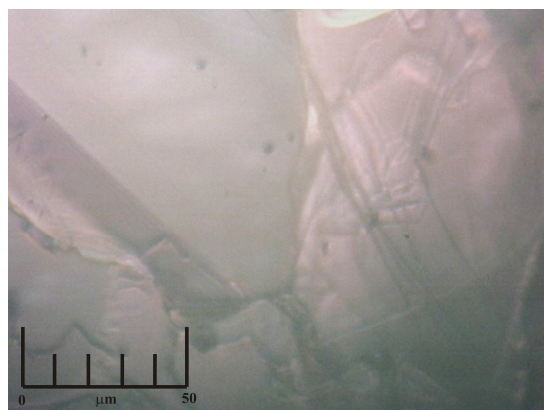


**Fig. 3** Microstructure of a ternary alloy in the three-phase region  $\alpha+\beta+\gamma$ .

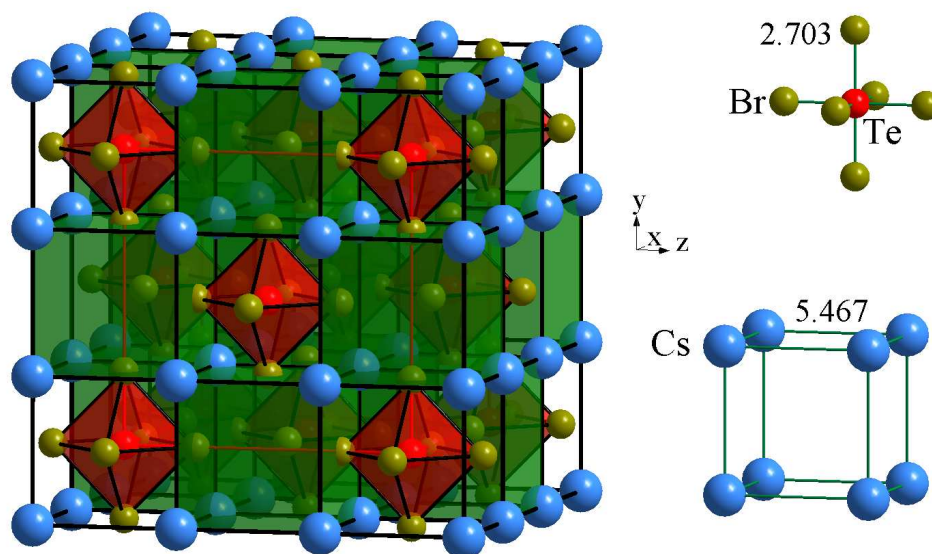


**Fig. 4** Stacking of empty (green) and filled (red octahedrons  $\text{TeX}_6$ ) cubes formed by Cs atoms, and interatomic distances  $\text{Te}-\text{Br}$  and  $\text{Cs}-\text{Cs}$  (Å), in the structure of  $\text{Cs}_2\text{TeBr}_6$ , *cF36*, 225.



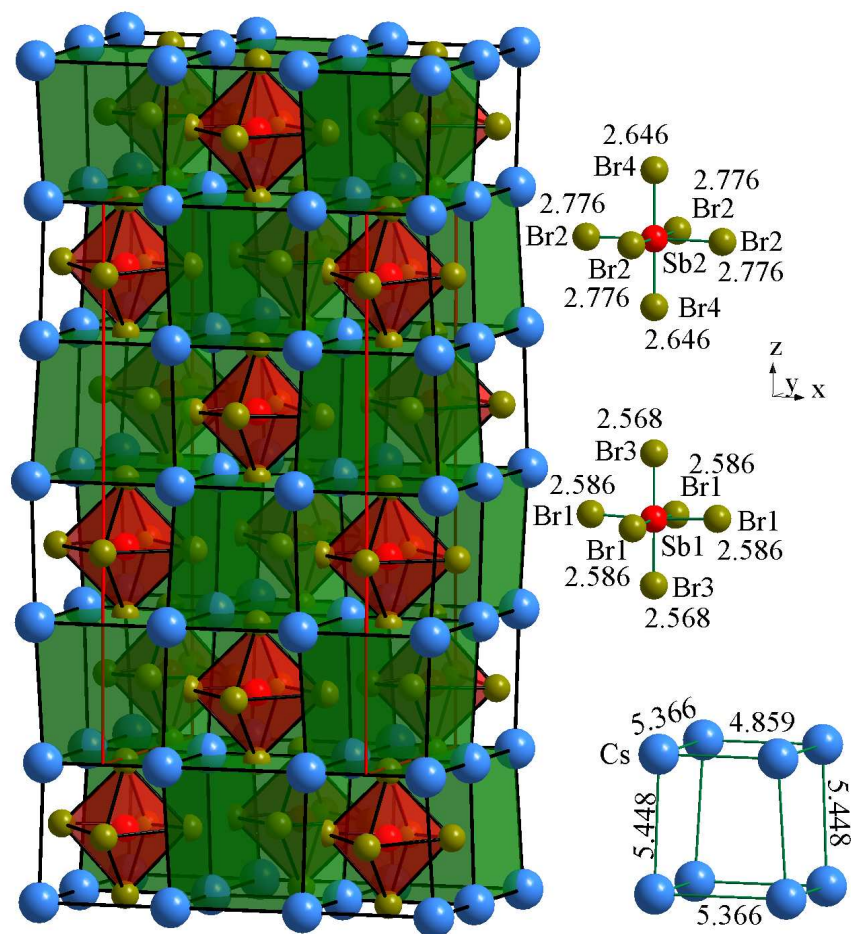


**Fig. 5** Stacking of empty (green) and filled (red octahedrons  $\text{SbX}_6$ ) cubes formed by Cs atoms, and interatomic distances Sb–Br and Cs–Cs (Å), in the structure of  $\text{Cs}_2\text{SbBr}_6$ , *tI72*, 141.

The compound *rtm*- $\text{Cs}_3\text{Sb}_2\text{Br}_9$ , *hP14*, 164 [26] crystallizes in the structural type  $\text{Cs}_3\text{Fe}_2\text{Cl}_9$ . The structure of this compound can also be represented as the stacking of cubes where the Sb atoms are surrounded by six Br atoms forming an octahedron  $[\text{SbBr}_6]$ . The octahedrons are interconnected by single Br atoms (Fig. 6).

The compound  $\text{Cs}_3\text{Sb}_2\text{I}_9$ , *hP28*, 194 [27] crystallizes in the structural type  $\text{Cs}_3\text{Cr}_2\text{Cl}_9$  (related to the previous structural types with the same composition and similar principles of construction). In the structure of the  $\text{Cs}_3\text{Sb}_2\text{I}_9$  compound, which can be represented as the stacking of merged cubes (Fig. 7), the Sb atoms are surrounded by six I atoms

and form  $[\text{SbI}_6]$  octahedrons. In the structure of this compound the  $[\text{SbI}_6]$  octahedrons are interconnected two by two by common faces.

The crystal chemical analysis shows that the interatomic distances between the Cs atoms that are located at the vertices of the cubes (forming empty and filled cubes in the structure) are increased in the order  $\text{Cs}_2\text{TeBr}_6$  (5.47 Å)  $\rightarrow$   $\text{Cs}_3\text{Sb}_2\text{Br}_9$  (5.51–5.82 Å)  $\rightarrow$   $\text{Cs}_3\text{Sb}_2\text{I}_9$  (5.93–5.99 Å). The presence of voids in the structures of the  $\text{Cs}_3\text{Sb}_2\text{Br}_9(\text{I}_9)$  and  $\text{Cs}_2\text{TeBr}_6(\text{I}_6)$  compounds makes it possible to form filled-in substitution derivatives on their basis, which can lead to the appearance of desired electrophysical and optical properties.

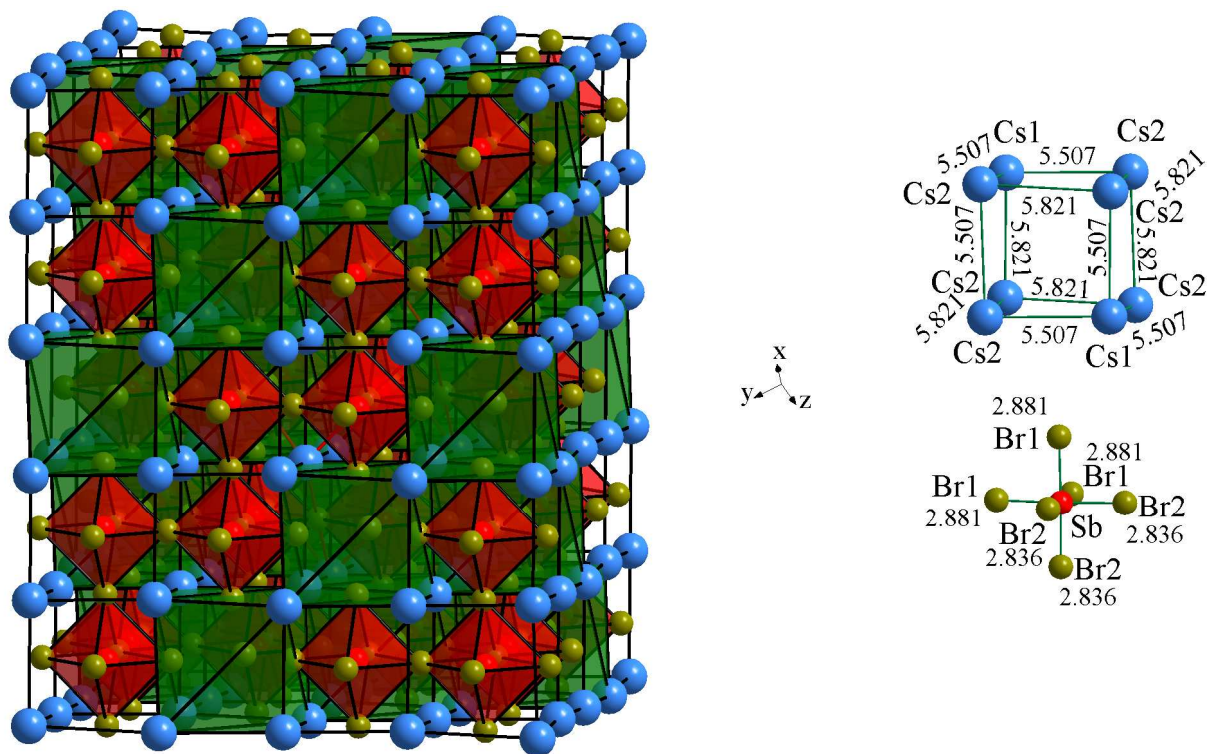


**Fig. 6** Stacking of empty (green) and filled (red octahedron  $\text{SbBr}_6$ ) cubes formed by Cs atoms, and interatomic distances Sb–Br and Cs–Cs (Å), in the structure of  $\text{Cs}_3\text{Sb}_2\text{Br}_9$ , *hP*14, 164.

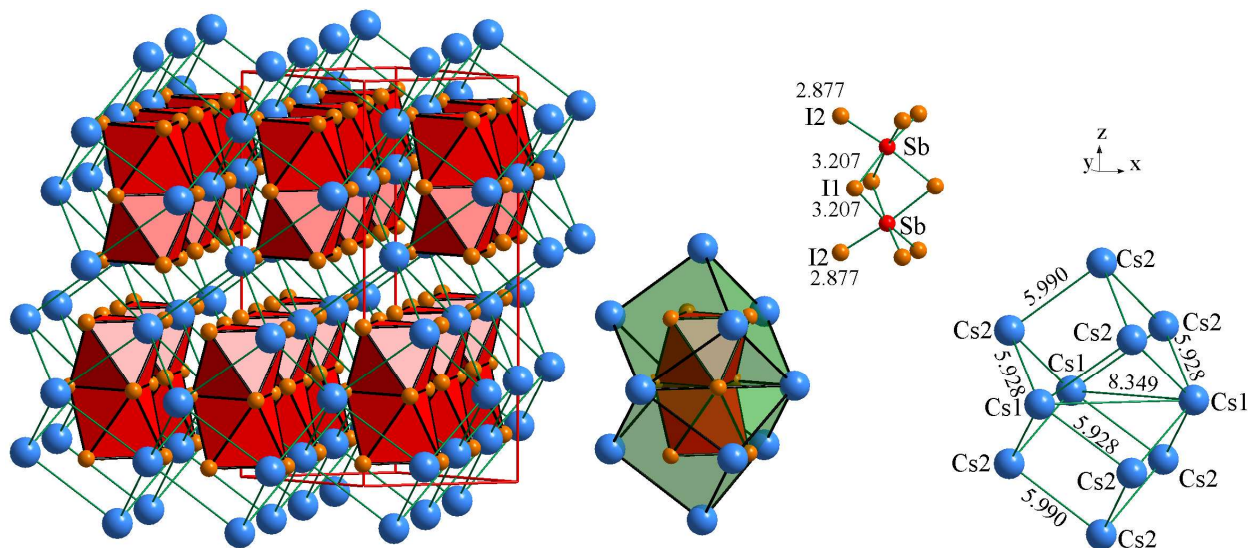


**Fig. 7** Stacking of face-sharing octahedrons  $\text{SbI}_6$ , merged cubes formed by Cs atoms, and interatomic distances Sb–I and Cs–Cs (Å), in the structure of  $\text{Cs}_3\text{Sb}_2\text{I}_9$ , *hP*28, 194.

## References

- [1] K.K. Ilyin, N.I. Nikurashina, *Zh. Prikl. Khim.* 53(10) (1980) 2111-2215.
- [2] N.J. Jeon, J.H. Noh, W.S. Yang, Y.C. Kim, S. Ryu, J. Seo, S.I. Seok, *Nature* 517(7535) (2015) 476-480.
- [3] D.P. McMeekin, G. Sadoughi, W. Rehman, G.E. Eperon, M. Saliba, M.T. Hörantner, A. Haghighirad, N. Sakai, L. Korte, B. Rech, M.B. Johnston, L.M. Herz, H.J. Snaith, *Science* 351(6269) (2016) 151-155.
- [4] R.J. Sutton, G.E. Eperon, L. Miranda, E.S. Parrott, B.A. Kamino, J.B. Patel, M.T. Hörantner, M.B. Johnston, A.A. Haghighirad, D.T. Moore, H.J. Snaith, *Adv. Energy Mater.* 6(8) (2016) 1502458.
- [5] D. Bi, B. Xu, P. Gao, L. Sun, M. Grätzel, A. Hagfeldt, *Nano Energy* 23 (2016) 138-144.
- [6] H. Choi, J. Jeong, H.-B. Kim, S. Kim, B. Walker, G.-H. Kim, J. Y. Kim, *Nano Energy* 7 (2014) 80-85.
- [7] C. Yi, J. Luo, S. Meloni, A. Boziki, N. Ashari-Astani, C. Grätzel, S.M. Zakeeruddin, U. Röthlisberger, M. Grätzel, *Energy Environ. Sci.* 9(2) (2016) 656-662.
- [8] Z. Li, M. Yang, J.-S. Park, S.-H. Wei, J.J. Berry, K. Zhu, *Chem. Mater.* 28(1) (2016) 284-292.
- [9] Xin-Gang Zhao, Ji-Hui Yang, Yuhao Fu, Dongwen Yang, Qiaoling Xu, Liping Yu, Su-Huai Wei, Lijun Zhang, *J. Am. Chem. Soc.* 139 (2017) 2630-2638.
- [10] A.J. Lehner, D.H. Fabini, H.A. Evans, C.-A. Hebert, S.R. Smock, J. Hu, H. Wang, J.W. Zwanziger, M.L. Chabinyc, R. Seshadri, *Chem. Mater.* 27 (2015) 7137-7148.
- [11] G. Volonakis, A.A. Haghighirad, R.L. Milot, W.H. Sio, M.R. Filip, B. Wenger, M.B. Johnston, L.M. Herz, H.J. Snaith, F. Giustino, *J. Phys. Chem. Lett.* 8 (2017) 772-778.
- [12] A.E. Maughan, A.M. Ganose, M.M. Bordelon, E.M. Miller, D.O. Scanlon, J.R. Neilson, *J. Am. Chem. Soc.* 138 (2016) 8453-8464.
- [13] N. Hara, F. Munakata, Y. Iwasaki, *J. Electrochem. Soc.* 145(1) (1998) 99-106.
- [14] C.A. Randall, A.S. Bhalla, T.R. Shrout, *J. Mater. Res.* 5 (1990) 829-834.
- [15] C. Li, X. Lu, W. Ding, L. Feng, Y. Gao, Z. Guo, *Acta Crystallogr. B* 64(6) (2008) 702-707.
- [16] I.P. Stercho, O.V. Zubaka, I.E. Barchiy, E.Yu. Peresh, O.P. Kokhan, A.I. Pogodin, *Nauk. Visn. Uzhhorod. Univ., Ser. Khim.* 1(37) (2017) 46-54.
- [17] V.G. Ziryanov, E.S. Petrov, *Izv. Akad. Nauk SSSR, Ser. Khim. Nauk B* 2(4) (1974) 109-111.
- [18] S.V. Kun, E.Yu. Peresh, V.B. Lazarev, A.V. Kun, *Neorg. Mater.* 27(3) (1991) 611-615.
- [19] E.Yu. Peresh, O.V. Zubaka, S.V. Kun, I.V. Galagovetz, I.E. Barchii, M. Yu. Sabov, *Neorg. Mater.* 37(8) (2001) 1000-1004.
- [20] E.Yu. Peresh, O.V. Zubaka, V.I. Sidey, I.E. Barchii, S.V. Kun, A.V. Kun, *Neorg. Mater.* 38(8) (2002) 1020-1024.
- [21] I.P. Stercho, I.E. Barchiy, E.Yu. Peresh, V.I. Sidey, T.O. Malakhovska, *Chem. Met. Alloys.* 6 (2013) 192-195.
- [22] I.P. Stercho, I.E. Barchii, T.A. Malakhovskaya, A.I. Pogodin, V.I. Sidei, A.M. Solomon, E.Yu. Peresh, *Russ. J. Inorg. Chem.* 60(2) (2015) 225-229.
- [23] E.Yu. Peresh, V.B. Lazarev, S.V. Kun, I.E. Barchiy, A.V. Kun, V.I. Sidei, *Neorg. Mater.* 33(4) (1997) 431-435.
- [24] E.Yu. Peresh, V.I. Sidey, O.V. Zubaka, *Neorg. Mater.* 41(3) (2002) 357-362.
- [25] I.E. Barchiy, *Ukr. Khim. Zh.* 67 (2001) 18-23.
- [26] S.V. Kun, V.B. Lazarev, E.Yu. Peresh, A.V. Kun, Yu.V. Voroshilov, *Izv. Akad. Nauk SSSR, Neorg. Mater.* 29 (1993) 410-413.
- [27] K. Yamada, H. Sera, S. Sawada, H. Tada, T. Okuda, H. Tanaka, *J. Solid State Chem.* 134 (1997) 319-325.
- [28] K. Prassides, P. Day, A.K. Cheetham, *Inorg. Chem.* 24 (1985) 545-552.
- [29] A.K. Das, I.D. Brown, *Can. J. Chem.* 44 (1966) 939-943.
- [30] L.M. Manojlovic, *Bull. Inst. Nuclear Sci. 'Boris Kidrich'* 6 (1956) 149-152.